

# Nonlinear, data-driven modeling of cerebrovascular and respiratory control mechanisms

Georgios D. Mitsis, *Member, IEEE*

**Abstract** — We present applications of recently developed algorithms for data-driven nonlinear systems identification to the study of cardiovascular and respiratory control mechanisms on an integrated systems level, utilizing experimental data obtained during resting conditions. Specifically, we consider cerebrovascular regulation during normal conditions in a two-input context, as well as respiratory control during a model opioid drug (remifentanyl) infusion in a closed-loop context. The results illustrate the potential of using data-driven modeling approaches, which do not rely on prior assumptions about model structure, for modeling physiological systems, as they are well-suited to their complexity. They also illustrate the potential of utilizing spontaneous physiological variability, which can be monitored noninvasively and does not require experimental interventions, to extract rich information about the function of the underlying mechanisms.

## I. INTRODUCTION

Homeostasis is maintained by the complex interaction of multiple mechanisms, which often involve feedback loops and inherent nonlinearities. As a result of these mechanisms and their constant interaction with a fluctuating environment, stochastic variations over a wide range of time scales arise in physiological signals. Consequently, resting physiological variability, contains rich information about the function of the underlying mechanisms under natural operating conditions. In this context, cardiovascular and respiratory control mechanisms are of particular importance. In the present paper we present the application of utilizing spontaneous physiological variability and nonlinear, data-driven systems identification to the investigation of these mechanisms. Specifically, we consider cerebrovascular regulation, as well as the investigation of the effects of opioid drugs on respiratory control.

The cerebrovascular bed is able to maintain cerebral blood flow (CBF) relatively constant despite changes in cerebral perfusion pressure [1]. Cerebral autoregulation was long viewed as a static phenomenon, whereby the “steady-state” pressure-flow relationship is described by a sigmoidal curve, suggesting that CBF remains constant despite changes in pressure within certain bounds. However, with the development of Transcranial Doppler (TCD) ultrasonography for the noninvasive measurement of CBF velocity (CBFV) with high temporal resolution, it was found that spontaneous CBFV variations may vary rapidly in response to variations of systemic arterial blood pressure

(ABP) [2]. Furthermore, the cerebrovascular bed is exquisitely sensitive to changes in arterial  $\text{CO}_2$  [1]. Spontaneous fluctuations of arterial  $\text{CO}_2$  tension, assessed by end-tidal  $\text{CO}_2$  ( $P_{\text{ETCO}_2}$ ) measurements, have a significant effect on slow fluctuations of both CBFV as well as regional blood flow, assessed by BOLD functional magnetic resonance imaging [3], [4]. It has also been suggested that cerebral hemodynamics are characterized by nonlinearities [2], [5]. Therefore, we have introduced a two-input, nonlinear model of cerebral hemodynamics [6], shown in Fig. 1, and in the present paper we show results obtained from using this model to study cerebrovascular regulation during resting conditions.

Much of the understanding of human respiratory control is based upon characterization of the ventilatory feedback loop, which is shown in Fig. 2 in a simplified form. Ventilatory responses are usually examined during hypoxic or hypercapnic stimulation [7]. Moreover, it has been shown that spontaneous breath-to-breath fluctuations in  $P_{\text{ETCO}_2}$  are responsible for a considerable fraction of the normal variability in tidal volume ( $V_T$ ) [8], and the dynamic effects of these spontaneous fluctuations have been used to derive information on ventilatory feedback [9]. Respiratory depression is the most common serious side effect of opioid drugs, [10], [11]; therefore, avoiding respiratory depression remains an important clinical aim. In the present paper we also considered the effects of a model opioid drug (remifentanyl) infusion on respiratory control by quantifying the dynamic interrelationships between  $P_{\text{ETCO}_2}$ ,  $V_T$  and breath-to-breath ventilation ( $V_T/T_{\text{TOT}}$ , where  $T_{\text{TOT}}$  is total breath time) in both causal directions of the ventilatory loop.

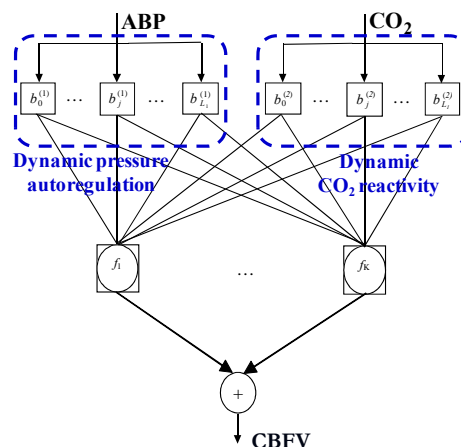


Fig. 1. Two-input, nonlinear model of cerebrovascular regulation, which includes the dynamic effects of ABP and arterial  $\text{CO}_2$  (assessed by  $P_{\text{ETCO}_2}$ ) on CBFV, termed dynamic pressure autoregulation and  $\text{CO}_2$  reactivity respectively.

Manuscript received August 25, 2009.

Georgios D Mitsis is with the Department of Electrical and Computer Engineering, University of Cyprus, Nicosia 1678, Cyprus (e-mail: gmitsis@ucy.ac.cy).

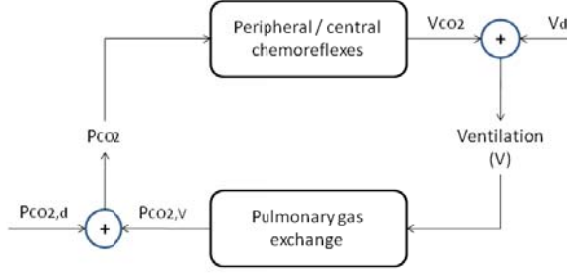


Fig. 2. Simplified diagram of the ventilatory feedback loop. Spontaneous ventilatory variability arises from a chemical component  $V_{CO_2}$  that is due to variations in  $CO_2$  variability  $P_{CO_2}$ , and a non-chemical component  $V_d$  (disturbance) due to all other physiological influences. Similarly, spontaneous  $P_{CO_2}$  variability arises from a ventilatory related component  $P_{CO_2,v}$  that is due to variations in  $V_T$  and a non-ventilatory related component  $P_{CO_2,d}$ .

## II. METHODS

The general Volterra model for a  $Q$ -th order nonlinear system with memory  $M$  in discrete time is:

$$y(n) = \sum_{q=0}^Q \sum_{m_1=0}^M \dots \sum_{m_q=0}^M k_q(m_1, \dots, m_q) x(n-m_1) \dots x(n-m_q) \quad (1)$$

where  $x(n)$  and  $y(n)$  are the system input and output respectively,  $M$  is the system memory and  $k_q(m_1, \dots, m_q)$  are the Volterra kernels of the system, which describe the linear ( $Q=1$ ) and nonlinear ( $Q>1$ ) dynamic effects of the input on the output. Among various methods that have been developed for the estimation of the Volterra kernels from input-output data, function expansions in terms of the orthonormal Laguerre basis has been proven to be particularly efficient:

$$k_q(m_1, \dots, m_q) = \sum_{j_1=0}^L \dots \sum_{j_q=j_{q-1}+1}^L c_{j_1 \dots j_q} b_{j_1}(m_1) \dots b_{j_q}(m_q) \quad (2)$$

where  $c_{j_1 \dots j_n}$  are the expansion coefficients,  $b_j(m)$  is the  $j$ -th order Laguerre function and  $L+1$  is the total number of functions that yields an adequate system representation. The coefficients can be efficiently obtained by ordinary least-squares [12].

We quantified the effects of remifentanyl on respiratory control in both directions of the ventilatory loop (Fig. 2). For the chemoreflex pathway ( $P_{ETCO_2} \rightarrow V$ ) sighs, which were defined as breaths with values greater than 1.5 times the mean breath value were removed by linear interpolation before model estimation, as they are viewed as part of the disturbance component of  $V$  ( $V_d$  in Fig. 1). A pure time delay of 2 breaths was hypothesized in the effects of  $P_{ETCO_2}$ .

The experimental data were collected from 11 healthy volunteers (age  $27 \pm 5$  years) during normal breathing and remifentanyl infusions of zero, 0.7, 1.1 and 1.5 ng/ml. Oxygen saturations, heart rate,  $P_{ETCO_2}$  and  $P_{ETO_2}$  were monitored continuously using a Datex Cardiocap II, while respiratory volume and timing was measured with a turbine respiratory flow meter. The baseline recordings were taken for 15 minutes. For each level of remifentanyl, five minutes were allowed to reach target effect site concentration;

continuous recordings were made for the following 15 minutes at that stable effect site concentration.

In the case of cerebrovascular regulation, we utilized the Laguerre-Volterra Network (LVN) model of Fig. 1, which combines Laguerre function expansions and networks with polynomial activation functions [6], [13]. The output of the two-input model of cerebrovascular regulation of Fig. 1 in terms of the MABP and  $P_{ETCO_2}$  inputs is given by:

$$CBFV(n) = k_0 + \sum_{i=1}^2 \sum_{m_1} k_{1x_i}(m_1) x_i(n-m_1) + \left\{ \sum_{i_1=1}^2 \sum_{i_2=1}^2 \sum_{m_1} \sum_{m_2} k_{2x_{i_1}x_{i_2}}(m_1, m_2) x_{i_1}(n-m_1) x_{i_2}(n-m_2) \right\} + \dots \quad (3)$$

where  $x_i$ : MABP,  $P_{ETCO_2}$ . The Volterra kernels  $k_q$  describe the linear and nonlinear effects of MABP and  $P_{ETCO_2}$  on CBFV and were used to quantify dynamic pressure autoregulation and  $CO_2$  reactivity ( $i=1$  and  $i=2$ ) respectively. The Volterra kernels in (3) can be expressed in terms of the LVN parameters, which are in turn estimated via an iterative gradient descent algorithm from the input-output data [13].

The experimental data were collected from 10 healthy subjects (age  $30 \pm 20$  years).  $P_{ETCO_2}$  was measured by mass spectrometry, ABP was monitored continuously in the finger by photoplethysmography and CBFV was measured with a 2-MHz Doppler ultrasound system in the right middle cerebral artery. The beat-to-beat values of ABP and CBFV and the breath-to-breath values of  $P_{ETCO_2}$  were interpolated and resampled at 1 Hz. Model estimation was performed using 6 min segments.

We used the normalized mean-square error (NMSE) of the output prediction to assess model performance in all cases. Model complexity was determined by the minimum description length criterion and by comparing the percentage NMSE reduction to the  $\alpha$ -percentile value of a  $\chi^2$  distribution with  $p$  degrees of freedom (where  $p$  is the increase of the number of free parameters and  $\alpha=0.05$ ).

## III. RESULTS

### A. Cerebrovascular regulation

The average achieved prediction NMSEs are given in Table I for one-input and two-input linear and nonlinear LVN models. ABP fluctuations explain most of the CBFV variations; however,  $P_{ETCO_2}$  reduced the NMSE significantly. A significant reduction in the prediction NMSE was also observed when nonlinear models were used [6]. Hence, the previously reported low coherence values between ABP and CBFV below 0.07 Hz are due to the effect of both nonlinearities and  $CO_2$ . This is illustrated in Fig. 3, where we show the decomposition of a representative model prediction into its linear and nonlinear, as well as into its ABP and  $CO_2$  components [6]. The model residuals in the frequency domain reveal that the contribution of these terms is more pronounced below 0.05 Hz. The first-order ABP and  $CO_2$  kernels, averaged over all subjects, are shown in Fig. 4. The high-pass characteristic of the linear ABP frequency response implies that autoregulation of pressure variations is more effective below 0.07 Hz. The linear first-order  $CO_2$

kernel exhibits a low-pass characteristic. Typical second-order MABP and CO<sub>2</sub> kernels are shown in Fig. 5, whereby most of their power lies below 0.1 Hz.

TABLE I  
CEREBROVASCULAR REGULATION DURING RESTING CONDITIONS: PREDICTION NMSES (MEAN±SD) FOR ONE-INPUT AND TWO-INPUT MODELS.

Model order	Model inputs [NMSE in %]		
	ABP	P <sub>ETCO2</sub>	ABP & P <sub>ETCO2</sub>
1	42.2 ± 7.2	93.2 ± 2.7	38.2 ± 6.5
2	25.7 ± 8.3	78.2 ± 25.7	22.0 ± 6.0
3	26.8 ± 7.6	71.7 ± 4.8	20.2 ± 5.4

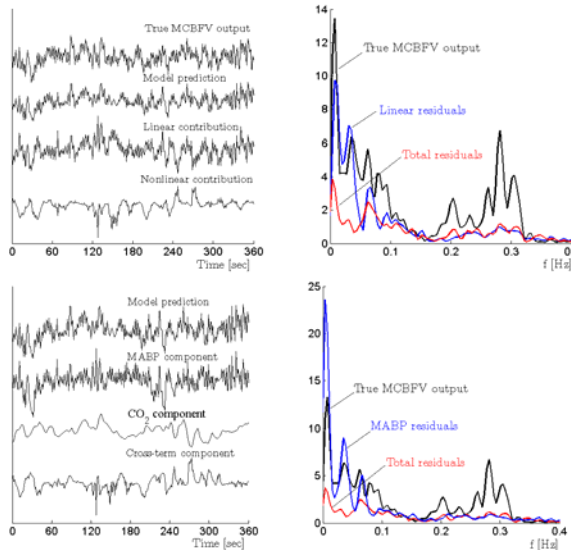


Fig. 3. Decomposition of model prediction of the two-input nonlinear model of cerebrovascular regulation into linear and nonlinear components, as well as into ABP and CO<sub>2</sub> components, for a representative data segment in the time (left) and frequency (right) domains - resting conditions.

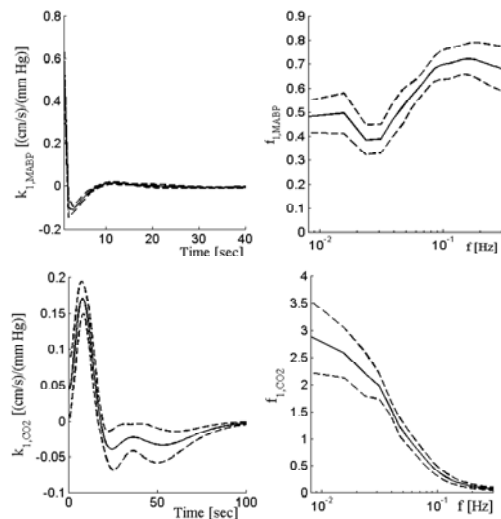


Fig. 4. First-order MABP and CO<sub>2</sub> kernels (solid lines) and corresponding standard errors (dotted lines), averaged over all subjects - resting conditions. Left panel: time domain, right panel: FFT magnitude.

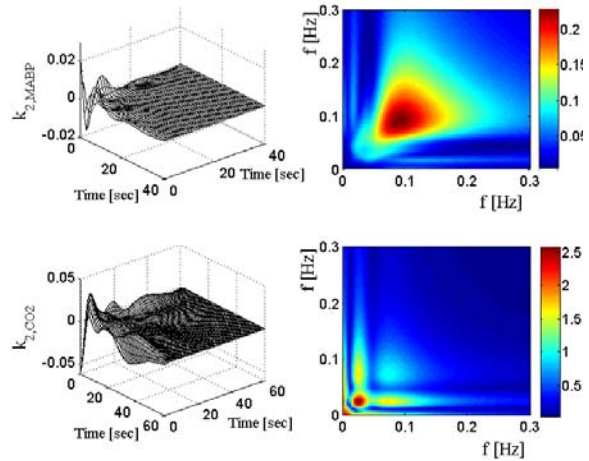


Fig. 5. Representative second-order MABP and CO<sub>2</sub> kernels. Left panel: time domain, right panel: 2D-FFT magnitude.

### B. Respiratory control during opioid infusion

The effects of remifentanyl on the respiratory variables were: (i) a dose-dependent decrease in respiratory rate that was due to increases in duration of expiratory time (TE) and its variability coefficient (see [15]) (ii)  $V_T$  initially decreased (at 0.7 ng/ml) but increased at higher levels towards baseline values and (iii) PETCO<sub>2</sub> increased and became more variable. The spectral power of PETCO<sub>2</sub> from 0 to 0.3 cycles/breath increased markedly, while  $V_T$  spectral power increased during remifentanyl infusion, albeit less pronouncedly above 0.02 cycles/breath. Nonlinear models reduced the prediction NMSEs significantly in both directions of the ventilatory loop [15]. Representative linear and nonlinear model predictions are shown in Fig. 6. PETCO<sub>2</sub> variations mainly account for the  $V_T$  post-sigh response, as sighs are clearly correlated with sharp PETCO<sub>2</sub> drops, which in turn influence  $V_T$ . These sharp drops are evidently accounted by the  $V_T \rightarrow$  PETCO<sub>2</sub> model. The incorporation of nonlinear model terms improved performance over a wide range of frequencies below 0.03 cycles/breath.

The averaged first-order kernels for the forward part of the ventilatory loop are displayed in Fig. 7, when both  $V_T$  (blue) and  $V_T/T_{TOT}$  (black) were used to assess ventilatory variability. Their form during baseline suggests that an increase in PETCO<sub>2</sub> will cause an increase in  $V_T$  (or  $V_T/T_{TOT}$ ), with the maximum instantaneous effects occurring at 4 and 8 breaths after the PETCO<sub>2</sub> increase. The kernel values decreased during remifentanyl, with the decrease being more evident for the second peak. For the reverse branch of the ventilatory loop ( $V \rightarrow$  PETCO<sub>2</sub>), the form of the first-order kernel suggests that an increase in ventilation will lead to a decrease in PETCO<sub>2</sub>, with the effects occurring almost instantaneously, i.e., within the first 2 breaths (results not shown). Remifentanyl infusion did not alter these characteristics; however, the kernel values increased at all levels, suggesting a stronger dynamic effect of ventilatory variability on PETCO<sub>2</sub>.

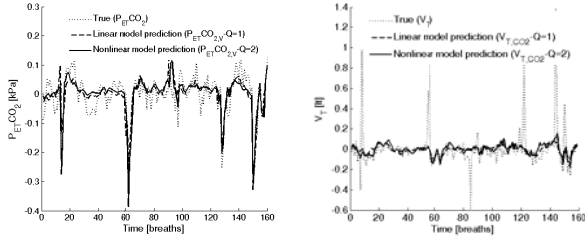


Fig. 6.  $P_{ETCO_2}$  (left panel - dotted line) and  $V_T$  (right panel - dotted line) time series during baseline, used for model estimation in both pathways of the ventilatory loop, and corresponding nonlinear model predictions ( $P_{ETCO_2,V}$  and  $V_{T,CO_2}$  respectively, solid lines).

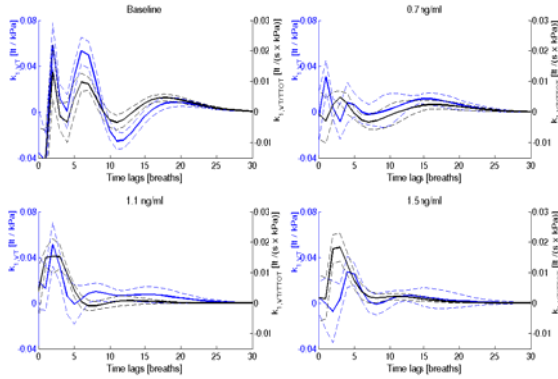


Fig. 7. Averaged first-order kernels for the chemoreflex pathway, whereby both  $V_T$  (blue) and  $V_T/T_{TOT}$  (black) were used to assess ventilatory variability. Remifentanyl decreased the impulse response values, particularly of the second peak.

The above observations are quantified by the spectral power of the first- and second-order kernels for both pathways shown in Fig. 8. For the chemoreflex branch (left), a decrease was observed in the spectral power of  $k_1$  and  $k_2$ . This decrease was statistically significant only during the lowest level of remifentanyl infusion for  $V_T$ ; however, more pronounced differences were observed when  $V_T/T_{TOT}$  was used as the model output. For the reverse pathway (right), the  $k_1$  spectral power increased significantly ( $P < 0.01$  during all remifentanyl levels for  $V_T$ ).

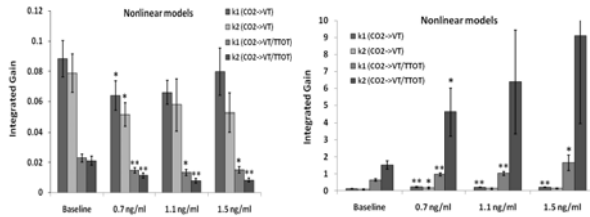


Fig. 8. Spectral power of the first and second-order Volterra kernels for the chemoreflex (left) and reverse (right) pathways. The spectral power of both the linear and nonlinear chemoreflex components between 0 and 0.3 cycles/ breath decreased during remifentanyl infusion. \*  $P < 0.05$ , \*\*  $P < 0.01$  compared to baseline.

#### IV. CONCLUSION

The presented results illustrate the potential of utilizing data-driven nonlinear modeling approaches to the study of cardiorespiratory regulatory mechanisms and, in a more general context, physiological systems on an integrated level. They also suggest that rich information regarding

system function can be extracted from spontaneous physiological variability, which does not require any experimental interventions and can be often readily measured in real life clinical situations. This approach, as shown in the cases considered above whereby the effect of experimental and pharmacological interventions on the system characteristics was studied, can also assess changes induced by such interventions, providing information about the contribution of different mechanisms that are involved. Consequently, our knowledge about system function during normal and pathophysiological conditions may be further enhanced and such approaches may be applied to diagnostic and therapeutic purposes.

#### ACKNOWLEDGMENT

The author would like to thank Profs. Marc Poulin, Peter Robbins, Rong Zhang Benjamin Levine and Dr. Kyle Pattinson for providing the experimental data.

#### REFERENCES

- [1] L. Edvinsson and D.N. Krause, *Cerebral Blood Flow and Metabolism*. Philadelphia, PA: Lippincott Williams and Wilkins, 2002.
- [2] R. Zhang, J.H. Zuckerman and B.D. Levine, "Spontaneous fluctuations in cerebral blood flow velocity: insights from extended duration recordings in humans," *Am. J. Physiol.* 278 (*Heart Circ. Physiol.*): H1848-1855, 2000.
- [3] Panerai, R.B., Simpson, D.M, Deverson, S.T., Mahony, P, Hayes, P and D.H. Evans, "Multivariate dynamic analysis of cerebral blood flow regulation in humans," *IEEE Trans. Biomed. Eng.* vol. 47, pp. 419-421, 2000.
- [4] R. G. Wise, K. Ide, M. J. Poulin, and I. Tracey, "Resting fluctuations in arterial carbon dioxide induce significant low frequency variations in BOLD signal," *Neuroimage*, vol. 21, pp. 1652-64, 2004.
- [5] G. D. Mitsis, R. Zhang, B. D. Levine, and V. Z. Marmarelis, "Modeling of Nonlinear Physiological Systems with Fast and Slow Dynamics. II. Application to Cerebral Autoregulation," *Ann. Biomed. Eng.*, vol. 30, pp. 555-565, 2002.
- [6] G. D. Mitsis, M. J. Poulin, P. A. Robbins, and V. Z. Marmarelis, "Nonlinear modeling of the dynamic effects of arterial pressure and  $CO_2$  variations on cerebral blood flow in healthy humans," *IEEE Trans. Biomed. Eng.*, vol. 51, pp. 1932-1943, 2004.
- [7] M.E. Pedersen, M. Fatemian and P.A. Robbins "Identification of fast and slow ventilatory responses to carbon dioxide under hypoxic and hyperoxic conditions in humans," *J Physiol* vol. 521, pp. 273-287, 1999.
- [8] M. Modarreszadeh and E.N. Bruce "Ventilatory variability induced by spontaneous variations of PaCO2 in humans," *J Appl Physiol* vol. 76, pp. 2765-2775, 1994.
- [9] J.G. van den Aardweg and J.M. Karemaker "Influence of chemoreflexes on respiratory variability in healthy subjects," *Am J Respir Crit Care Med* 165: 1041-1047, 2002.
- [10] K.T. Pattinson "Opioids and the control of respiration," *Br J Anaesth* vol. 100, pp. 747-758, 2008.
- [11] N.M. Mellen, W.A. Janczewski, C.M. Bocchiaro and J.L. Feldman "Opioid-induced slowing reveals dual networks for respiratory rhythm generation," *Neuron* vol. 37, pp. 821-826, 2003.
- [12] V.Z. Marmarelis "Identification of nonlinear biological systems using Laguerre expansions of kernels," *Ann Biomed Eng* 21: 573-589, 1993.
- [13] G.D. Mitsis and V.Z. Marmarelis, "Modeling of nonlinear systems with fast and slow dynamics. I. Methodology," *Ann. Biomed. Eng.*, vol. 30, pp. 272-281, 2002.
- [14] G.D. Mitsis, R. Zhang, B. D. Levine, and V. Z. Marmarelis, "Cerebral hemodynamics during orthostatic stress assessed by nonlinear modeling," *J Appl Physiol*, vol. 101, pp. 354-66, 2006.
- [15] G.D. Mitsis, R.J. Governo, R. Rogers and K.T. Pattinson, "The effect of remifentanyl upon respiratory variability, evaluated with dynamic modeling," *J Appl Physiol*, vol. 106, pp. 1038-1049, 2009.